4-2016

Nicotine-Mediated ADP to Spike Transition: Double Spiking in Septal Neurons

Sodikdjon A. Kodirov
The University of Texas Rio Grande Valley

Michael Wehrmeister

Luis V. Colom
The University of Texas Rio Grande Valley

Recommended Citation

Kodirov, S.A., Wehrmeister, M. & Colom, L. Nicotine-Mediated ADP to Spike Transition: Double Spiking in Septal Neurons. J Membrane Biol 249, 107–118 (2016). https://doi.org/10.1007/s00232-015-9853-2

HHS Public Access

Author manuscript

J Membr Biol. Author manuscript; available in PMC 2017 June 20.

Published in final edited form as:

J Membr Biol. 2016 April ; 249(1-2): 107–118. doi:10.1007/s00232-015-9853-2.

Nicotine-Mediated ADP to Spike Transition: Double Spiking in Septal Neurons

Sodikdjon A. Kodirov[1,2], **Michael Wehrmeister**[3,4], and **Luis Colom**[1]

[1]Department of Biological Sciences, Center for Biomedical Studies, University of Texas at Brownsville, Brownsville, TX 78520, USA

[2]Neuroscience Institute, Morehouse School of Medicine, 720 Westview Drive SW, Atlanta, GA 30310, USA

[3]Johannes Gutenberg University, 55099 Mainz, Germany

Abstract

The majority of neurons in lateral septum (LS) are electrically silent at resting membrane potential. Nicotine transiently excites a subset of neurons and occasionally leads to long lasting bursting activity upon longer applications. We have observed simultaneous changes in frequencies and amplitudes of spontaneous action potentials (AP) in the presence of nicotine. During the prolonged exposure, nicotine increased numbers of spikes within a burst. One of the hallmarks of nicotine effects was the occurrences of double spikes (known also as bursting). Alignment of 51 spontaneous spikes, triggered upon continuous application of nicotine, revealed that the slope of after-depolarizing potential gradually increased (1.4 vs. 3 mV/ms) and neuron fired the second AP, termed as double spiking. A transition from a single AP to double spikes increased the amplitude of after-hyperpolarizing potential. The amplitude of the second (premature) AP was smaller compared to the first one, and this correlation persisted in regard to their duration (half-width). A similar bursting activity in the presence of nicotine, to our knowledge, has not been reported previously in the septal structure in general and in LS in particular.

Keywords

Lateral septum; HCN channels; Action potentials; ADP; Double spikes; AHP

> …in the hippocampal formation and septum, clear behavioral correlates can be determined for almost all neurons…
>
> Ranck, 1973

Introduction

The septal structure of the brain has several inputs and outputs, and major ones could be considered to and from the hippocampus. Stimulation of hippocampus suppresses the

Correspondence to: Sodikdjon A. Kodirov.

[4]Present Address: Heidelberg University, Heidelberg, Germany

activity of neurons in the lateral septum (LS), which receives outputs from CA3 regions via *fornix precomissuralis* (Vinogradova 2001). LS neurons are also prone to long-term potentiation (LTP) that can be induced by the stimulation of *fornix* (Racine et al. 1983; van den Hooff et al. 1989). Stimulation of CA1 pyramidal layer of the hippocampus in addition results in LTP of neurotransmission in septal neurons. This is a reciprocal phenomenon, i.e., the stimulation of septum induces LTP in CA1 pyramidal neurons; the latter also leads to potentiation in the subiculum and amygdala. The stimulation of *fimbria* triggers excitatory neurotransmission (van den Hooff et al. 1989), and upon adequate paradigm leads to vasopressin dependent LTP in LS. The hippocampus possesses a local and dedicated inhibitory drive, but the GABAergic signals sent by the septum can dominate and lead to the disinhibition of pyramidal neurons of CA1/3 regions and granular cells of dentate gyrus (Freund and Antal 1988). Disinhibition of principal cells is not triggered directly by the GABAergic neurons of the septum, but via their inhibitory effects on hippocampal interneurons (Toth et al. 1997).

There are a few studies dedicated to LS (Carette 1999; Thomas et al. 2013) because of the lack of direct synaptic inputs into the hippocampus. We have recently described the hyperpolarization-activated cyclic nucleotide (HCN or I_h) gated non-selective cation channels in LS (Kodirov et al. 2014). The very first hint for existence of these channels and their involvement in pace-making was evidenced in Purkinje fibers and was termed i_{K2} (Noble and Tsien 1968). The discovery of i_{K2} subsequently underwent extensive interpretations by these and other authors (Vassalle et al. 1995). Recurrent activation of HCN channels (DiFrancesco et al. 1991; Luthi and McCormick 1998) leads to rhythmic spiking in diverse cells (Mao et al. 2003; Pal et al. 2003), and during developmental stages of the brain it triggers GDP—giant depolarizing potentials (Bender et al. 2005). Both the involvement of HCN to and its altered expression in seizures depend on specific brain areas and underlying subunits/isoforms (Adams et al. 2009). HCN channels are progressively activated by hyperpolarization, do not inactivate during at least seven seconds (Thon et al. 2014), are sensitive to cocaine (Campanac and Hoffman 2013), and contribute to septohippocampal memory processing (Cisse et al. 2008).

An addiction to nicotine (Changeux 2009) occurs in the brain by targeting neurons and nicotinic acetylcholine receptors (nAChR). There is a crucial difference between the neuronal nAChRs and those of other cell types in terms of their distribution in the membrane and endoplasmatic reticulum (D'Agostino et al. 2014). The intravenous nicotine injection (Mameli-Engvall et al. 2006) increases the action potential rate and numbers of spikes within a burst (SWB). Similar response of dopaminergic (DA) neurons in the ventral tegmental area (VTA) persisted in $\alpha7^{-/-}$, but not in $\beta2^{-/-}$ mice. Nicotine has been shown also to increase the frequency of spikes (by ~75 %) in tonically active cholinergic medial habenular (MHb) neurons (Görlich et al. 2013). Although the nAChR composed of $\alpha3\beta4$ were defined as an excitatory mediator, only mecamylamine (MEC) prevented the effects of nicotine, while dihydro-β-erythroidine (DHbE), 3-(4)-dimethylaminobenzylidine anabaseine (DMAB), and bungarotoxin decreased it to ~50 %, conotoxin AuIB or SR 16584 inhibited to ~20 %, and conotoxin MII had no effects.

It is emerging that nicotine has additional targets, i.e., it modulates HCN channels (Kodirov et al. 2014). Furthermore, our pharmacological characterization using antagonists for multiple subunits of nAChR revealed that the HCN channels were directly modulated by nicotine. The current study focuses on main properties of spontaneous and evoked APs and the mechanism underlying the double spiking triggered by nicotine in LS.

Results

We have experimented with neurons of LS (Fig. 1) by focusing on parameters of APs, which were always either recorded at (spontaneous spikes, Figs. 2, 3, 4, 5, 6, 7, 8 and 12) or evoked from the RMP (−60.6 ± 2 mV, $n = 21$) by injection of constant depolarizing currents of up to 300 pA (Figs. 9, 10 and 11). Under control conditions, only in 5 out of 19 cells did we observe spontaneous activities. These differences correlated with the mean values of RMP in two groups: −48.5 ± 4 versus −62 ± 1.5 mV ($P < 0.001$), respectively. These cells comprise only those to which subsequently nicotine at least at one of concentrations (0.3, 1, and 3 μM) was applied.

Basal Electrical Activity of LS Neurons

In order to elucidate the effects of nicotine in the LS, we first have continuously observed activity of neurons at RMP for longer periods. The inhibitory and excitatory drive in the slice was undisturbed in this case. Under control conditions (i.e., ACSF alone), most of the neurons did not exhibit spontaneous APs or in a rare case a few spikes within minutes could be observed (Fig. 2a). Application of nicotine at 1 μM concentration led to a transient depolarization accompanied by a few APs (Fig. 2b). Thereafter, the neuron was silent and similarly responded to the next cumulative concentration of nicotine. Upon the continuous presence of 3 μM nicotine, the neuron generated relatively regular spikes/bursts (Fig. 2c). Data revealed that the amplitudes of these APs were smaller (Fig. 2c) compared to those few observed both under control conditions (Fig. 2a) and in the presence of 1 μM nicotine (Fig. 2b). These effects are easy to discriminate when the overshoot potentials are compared (26.7 ± 0.2 vs. 18.8 ± 0.3 and 6.6 ± 0.2 mV, respectively), although the RMP was slightly negative after application of nicotine (Fig. 2b, c) and during the course of wash-out (Fig. 2d). The effect of nicotine on overshoot potential was to some extent reversible (13.7 ± 0.4 mV), but the bursting persisted during a 30-min wash-out. These mean values were estimated from 2, 4, 60, and 54 APs, respectively, for conditions presented in Fig. 2. The properties of APs within the burst resembled those of evoked ones (see Fig. 9), specifically the occurrence of “double spikes” at the beginning of each burst (Fig. 2c). This phenomenon was not seen under control conditions (Fig. 2a). Occasionally just only double spiking (without conventional bursting) was observed in the presence of nicotine (Fig. 2c). After-depolarizing potentials (ADP) were observed upon the termination of the repolarization phase of single spikes only (Fig. 2a, b and d). During the burst, the MP remained depolarized and subsequently repolarized back to initial RMP value upon its termination. The nicotine triggered bursting mode had a frequency of 0.16 ± 0.02 Hz (Fig. 3a–c). In this and in Figs. 4, 5, 7 and 8 each vertical bar represents an AP recorded in real time. The frequencies of both bursting and double spikes were not sensitive to longer applications of up to 18 min (Fig.

3c). The rate of the majority of spikes is centered at ~1 Hz (however, see Fig. 4), while the frequency around 100 Hz reflects double spiking.

Double Spikes

Since both the sequential timing of first three spikes and their amplitude within the burst are not similar (Fig. 4), it is not straight forward to define double spikes as the 1st and 2nd APs. The analyses reveal that a double spiking in LS is not preprogrammed, but an opportunistic phenomenon depending on the magnitude of ADP (see Fig. 6) in those neurons exhibiting such a component of AP. During continuous perfusion of nicotine, we have observed seven bursts/min^{-1} and three are presented in sequential order in Fig. 4a–c. The frequencies of bursts and SWB could be clustered into the three diapasons: the burst, subsequently the 1st AP is triggered at 0.1–1 Hz, the double spikes, i.e., the 2nd AP at 100–200 Hz, and the 3rd and following spikes at 1–10 Hz. This pattern of spiking could be described as adaptation in frequency and amplitudes of APs. Interestingly, the absence of double spiking (indicated with **I** as a predicted 2nd AP, Fig. 4c) does not obliterate the sequential frequencies of SWB.

The amplitudes of all SWB vary, but they mirror the bursting behavior of neurons (Fig. 5a–c). In contrast to the frequency values, only two clear diapasons for the amplitude are distinguished. The first one is either the amplitude of single spikes, or the 1st, 3rd and subsequent SWB (Single). The next diapason comprises the magnitude of the 2nd AP during double spiking (Double), and which is lower than those of first group. Why does their amplitude (also duration) vary transiently? The most plausible explanation: the 2nd AP is triggered prematurely by a transition from the ADP (Fig. 6). This notation is substantiated by an increase in the slope of ADP (1.4 vs. 3 mV/ms) after the exposure to nicotine. Smaller amplitudes of 2nd spikes are presumably a result of both incomplete inactivation and activation of Nav1 channels.

Phenomenon ADP during evoked APs might have some peculiar features in LS. (1) The ADP either is selectively locked/related to the 1st AP during up to 1 s depolarization, (2) or similar to APs is also prone to a refractory period, (3) or starting with the 2nd AP, the after-hyperpolarizing potential (AHP) dominates the ADP and masks it. The 3rd possibility is unlikely, since an ADP always precedes the AHP (Fig. 6b), at least its slow component (sAHP). Nicotine increases the ADP, which in turn triggers the 2nd premature spike (Fig. 6c). Thus, the underlying mechanism for the 2nd AP is a simple ADP to spike transition (AP ← ADP). Note that the overshoot potential is low for the 1st spikes, because of the effects of nicotine (see Fig. 2c).

In contrast to the evoked train of APs in LS neurons, every single spontaneous spike possesses an ADP and thus their values also mirror the above-mentioned bursting behavior (Fig. 7a–c). By including the amplitudes of the 2nd spikes, we show that they logically do not trigger ADP (*blue-colored down arrow*, Fig. 7c, and see Fig. 6c), but they increase the amplitude of AHP (Double, Fig. 8). There was a moderate linear relationship between the AHP triggered by one AP (Single, Fig. 8) and those by fewer double spikes. A similar dependency persisted in respect to frequencies of SWB during the three 1-min sequential recordings (Fig. 8a–c). The degree of linear relationship was less pronounced when amplitudes of SWB were compared (data not shown), but were comparable. Phenomenon

AHP (Figs. 6, 8) is not only a product of Na^+-dependent spikes, but also Ca^{2+}-mediated ones. Accordingly, their time course is very slow (sAHP) and ranges up to ~5 s in the thalamus (Kolaj et al. 2014). Nevertheless, the sAHP is observed only in the presence of extracellular Na^+ and the substitution with Tris eliminates it, but lithium transforms it into an even slower ADP. Note that also the duration of AHP in LS (>100 ms, Fig. 6) similar to amygdalar and striatal ones (Kodirov et al. 2006; Ponterio et al. 2013) is considered slow despite much a shorter duration compared to that in the thalamus. The fast AHP lasting only ~10 ms are observed in granular cells of dentate gyrus (Kodirov, unpublished).

Nicotine Effects on Latency

At the beginning of this study, one of the aims was to compare the latencies (before reaching a threshold) of spontaneous and evoked APs. Since the spontaneous and recurrent APs occurred only in a minority of neurons, we next analyzed the latencies for AP generated during injected pulse of currents (Fig. 9). When APs are evoked by somatic current injections, double spikes appear at more depolarized states and their frequency increases accordingly (Fig. 9). The same is true for the amplitude of the 1st AP during each step and the double spikes may reflect the state of increased excitability.

Also in this set of experiments, we have compared and analyzed the effects of nicotine in the same neurons. In four out of 8 cells the time to threshold in the presence of 3 μM nicotine significantly decreased by 61.2 ± 15.5 % of control ($n = 4$, Fig. 10a–c). Under identical conditions, nicotine slowed down the time course in remaining cells by 267.8 ± 88.2 % ($n = 4$, Fig. 10d). Next, a consistent observation was made in regard to timing to the 1st AP at (for example) 20 pA and the subsequent ones evoked by depolarizing steps ranging up to 300 pA. Under control conditions (Fig. 10e), the latency for AP at rheobase and subsequent incremental (20 pA) current injection were 168 ± 38.1 and 77.8 ± 15.3 ms ($n = 8$), respectively. Application of nicotine (Fig. 10f) did not significantly affect the latter values and a similar tendency persisted (137.4 ± 35.7 and 76.2 ± 19.2 ms, $n = 8$, $P = 0.3$ and $P = 0.9$ for both corresponding control values). In the absence (Fig. 10e) and presence of nicotine (Fig. 10f), the ratio of the time to thresholds between the 1st injected current magnitude and 2nd one (e.g., AP at 40 pA/AP at 20 pA that depends on the actual threshold of individual neuron) was 0.5 ± 0.04 and 0.58 ± 0.03 ($n = 8$, $P = 0.1$, paired t test), respectively. This ratio of AP latencies between those evoked/obtained by subsequent incremental current magnitudes was not dramatic and has slowly stabilized (Fig. 10e, f).

Correlation of Amplitudes and Widths of Spikes Behaviors

Next, we were interested in whether or not the nicotine, under identical conditions, will affect the active properties of the membrane/neuron. We have observed that in a majority of cells the amplitude of a 2nd AP at given injected current magnitude was always smaller and it either gradually further decreased or abruptly reversed toward the value of 1st AP (Fig. 11a, b). The latter phenomenon could be considered as “complex spikes” (Ranck 1973) and was dependent upon the magnitude of injected currents. For example, in the particular neuron shown in Fig. 11a (at 40 pA) and Fig. 11b (140 pA) the amplitudes of seven subsequent APs evoked by current magnitudes ranging between 40 and 100 pA gradually decreased in comparison to the very 1st AP (Fig. 11c). For clarity in y axes only the actual

range is shown by introducing break points. The APs evoked by 120, 140, and 160 pA steps (Fig. 11c) behave differently and show a significant and transient decrease in amplitude of 2nd AP. Interestingly, the amplitude of 3rd AP had a similar value as the 1st one and the following APs obey a gradual rule. Note that in this neuron the injection of 20 pA current was not sufficient (at least during 1 s) to depolarize the MP up to the threshold. Finally, there was a clear correlation between the decreased amplitude and the increased duration (half-width) of the 2nd AP at all injected current magnitudes (Fig. 11d). Also the half-widths of APs have increased either abruptly or gradually.

Application of nicotine to the same neuron both decreased the amplitude and resulted in greater variability of amplitudes of APs (Fig. 11e). In the presence of nicotine, the LS neuron responds with the decreased amplitude of the 2nd AP compared to all spikes evoked by 40 pA (Fig. 11e). These particular effects of nicotine have impact on up to the first 4 APs (Fig. 11f). The magnitude of 2nd, 3rd, and even 4th APs evoked by 140 pA remained significantly lower before almost completely reversing to amplitude values of 1st ones as illustrated (Fig. 11f). Normalized values (the amplitude of 1st AP as reference) revealed a comparable phenomenon also for APs evoked by 20–160 pA (Fig. 11g). Importantly, the latter effects of nicotine were mirrored also in regard to half-widths of APs (Fig. 11h). Note that a decrease in the amplitude of APs (Fig. 11g) and prolongation of their durations (Fig. 11h) in the presence of nicotine were not gradual. Nicotine presumably influences the underlying cellular mechanism for ADP, and the resultant increase in intracellular Ca^{2+} decreases the amplitudes of subsequent up to three APs (Fig. 11g) and prolongs their durations (Fig. 11h). A decrease in amplitudes of spikes mainly results from the effects of nicotine on over-shoot potential (Fig. 12). The analyses of ΔmV/Δms revealed that the waveforms of 1st APs during either a single ($n = 35$) or double spiking ($n = 10$) are not apart (Fig. 12c, d, respectively). These results are consistent with a notion that the 2nd spike is a product of upregulated ADP by nicotine, but is not triggered by the 1st AP per se.

Discussion

Several lines of evidence suggest that nicotine can act synergistically with other neurotransmitters including ACh (Fisher and Dani 2000), and it facilitates both the GABA and glutamate release (Bancila et al. 2009). However, in LII/III of the frontal cortex, nicotine increased the inhibitory neurotransmission but not the excitatory one (Klaassen et al. 2006). Nicotinic ACh receptor agonism excites (enables the generation of additional APs) the distinct types of interneurons of neocortex that results in subsequent enhancement of GABA release and thereby in additive inhibition (Porter et al. 1999). Nicotine effects on both frequency and numbers of SWB in VTA DA neurons outlasted for minutes (not ~1 s as indicated by the graph) after injection and were completely reversible within ~15 min (Mameli-Engvall et al. 2006).

Its capability of interaction with known neurotransmitters points that nicotine could also control additional elements of neurons. Note that nicotine has dual effects (excitatory and inhibitory) on evoked APs (Kodirov et al. 2014), which is mediated via modulation of HCN channels and should theoretically pertain also in the case of spontaneous spikes. However, precautions are warranted, since HCN shares conserved α B-helix regions with K^+ channel

and some antagonists inhibit I_h and K^+ currents or even Cav1 channels with overlapping affinities (Nazzari et al. 2008; van Welie et al. 2005; Vasilyev et al. 2007).

In the current study, we have evidenced that nicotine triggers spontaneous APs, and upon frequent recurrent activities a bursting mode is observed. Detailed analyses revealed that the frequency behavior of spontaneous spikes within each burst is both predictable and compensated when the 2nd spike is absent (**I**, Fig. 4d). We also evidenced that the 2nd AP could be evoked by nicotine and there is a clear ADP to spike transition derived from the increased slope and amplitude (Fig. 6). We suggest that the underlying mechanism could involve Ca^{2+} influx enabled by HCN channels. Although the effects of nicotine on I_h are most striking, involvements of other voltage-dependent and -independent ion channels can not be ruled out. Thus, the experimentally observed “nicotine effects can not be only attributed to its multiple receptors, and no single brain area is a definitive target” (Kodirov 2015).

HCN channel contribution could reliably be manifested by hyperpolarization in voltage- and current-clamp modes in the same LS neuron (Kodirov et al. 2014). Precise patterns of activation are also shown for single HCN2 channels in cell-attached and inside-out modes (Thon et al. 2014). Most of channels are readily open within the first seconds of hyperpolarization and do not transit into the closed state. Interestingly, cAMP was able to activate only one additional channel under these conditions, and single channel conductance remained unaffected at the ~1.6 pS level. Note that the facilitation of the opening of HCN2 channels by cAMP is considered stronger compared to HCN1 (Rozario et al. 2009). Nevertheless, the waveforms of I_h and underlying sag in a variety of cells, including retinal rods, are very similar (Mao et al. 2003). It has been elegantly shown that the magnitude of I_h depends on internal K^+ salts, which is smaller with K^+-gluconate (Velumian et al. 1997). However, K^+-gluconate in current-clamp mode increases the sag, which perhaps was overlooked, since the purpose of those particular experiments was different as stated: “voltage transients in response to hyperpolarizing current steps had a depolarizing sag that affected the precise estimation of membrane input resistance.”

The deletion of one so far known auxiliary subunit of HCN channels—tetratricopeptide containing Rab8b-interacting protein (TRIP8b)—eliminates the sag and resultant rebound tail potential (RTP) in neurons of the CA1 region of the hippocampus (Brager et al. 2013; Lewis et al. 2011). These effects are paralleled by an increased excitability upon the depolarization in TRIP8b$^{-/-}$ mice. Note that the changes in excitability (Brager et al. 2013; Lewis et al. 2011) are strictly dependent on the magnitude of injected depolarizing currents, since in the same transgenic animals and neuronal type, the properties of evoked APs by theta burst train did not differ (Brager et al. 2013). All four HCN α subunits are expressed in the brain (Brauer et al. 2001; Day et al. 2005), and thus the effects of I_h, each subunits, antagonists, and agonists are much more complex than in many previously described studies. This includes also the dual effects of nicotine on HCN channels: (1) inhibition of sag and RTP, and an increased firing rate may occur in parallel (Koch and Grothe 2003), (2) elimination of sag and RTP does not necessarily change the excitability (Thuault et al. 2013), (3) an increase in sag may lead to RTP into RAP transition, which is accompanied by facilitated excitability upon the depolarization, (4) over-activation of HCN channels will

increase the sag potential, but diminishes the excitability of neurons. HCN channels are differentially expressed in prekaryon and dendrites, and the magnitude of sag and RTP in the soma of CA1 neurons are lower (Brager et al. 2013; Lewis et al. 2011). RTP sometimes is cited as a transient overshoot that occurs due to deactivation of I_h (Solomon et al. 1993). The summation of EPSPs (to which HCN channels contribute) in dendrites are lower and results from higher levels of HCN expression (Magee 1999). The sag kinetics in CA1 pyramidal cells are faster (Brager et al. 2013) compared to LS neurons (Kodirov et al. 2014), which may well reflect differences in subunit expressions as demonstrated for neurons of vomeronasal organ (VNO) in mice (Dibattista et al. 2008).

The sag is not always considered to be driven by I_h and occasional studies have found supporting evidence. In one of them, both the sag and expression of HCN1 were decreased by TTX (Arimitsu et al. 2009). The recurrent activation of HCN channels can also lead to spontaneous sag during the down states followed by long plateau potentials as shown for inhibitory NRT (nucleus reticularis thalami) neurons (Blethyn et al. 2006). In contrast, in pyramidal neurons of layer V of mPFC the deletion of HCN1 had no impact on these two states or on excitability in vivo (Thuault et al. 2013).

Neurons of the LS may play an important role alone by the fact that they are exposed to *liquor cerebrospinalis* (McRae-Degueurce et al. 1987) of ventricles—*cavum septi pellucidi* (CSP). Dramatic changes should occur in this fluid during diseases, which could affect the properties of LS neurons, at least those located most dorsally. In addition, it is perhaps important to study this area, since activity of LS neurons are relayed to the CA3 as the element of hippocampal regulatory circuit (Vinogradova 2001). In LS, similar to evoked APs (Kodirov et al. 2014), the amplitude of spontaneous spikes also decreased in the presence of nicotine. The underlying mechanism is not clear, but the number of activated channels may contribute to increased APs frequency paralleled by a decrease in their amplitude (Kononenko and Berezetskaya 2010). Nicotine also comparably diminishes the amplitude of local field potentials, but increases their frequencies (Matsuo et al. 2014).

Our results shed additional light on nicotine effects and bursting properties of LS neurons in general, and the behavior of amplitude, ADP, AHP, frequency, latency, and width of APs in the brain in particular. Since the timing of ADP and “double spikes” match closely after application of nicotine, we concluded that they are inter-related events (Fig. 6b, c). The bursting mode in the presence of nicotine is HCN channel dependent, and this notion is supported by the basics of mitral cells properties (Angelo and Margrie 2011). These neurons also could be subdivided into the two groups by the absence and presence of sag. Importunately, cells lacking the sag possess a bursting behavior, which was also observed when the sag was blocked by ZD 7288. An ADP into spike transition at relatively low concentration of nicotine may functionally play a role during the synergistic synaptic (and spike) plasticity and related behavior in the septo-hippocampal complex. HCN apparently plays a role not only in memory, but also in long-term depression (Tokay et al. 2009). Moreover, because of the established involvement of HCN channels in epilepsy (Marcelin et al. 2009), nicotine effects could enable a targeted modulation at neuronal level. Nevertheless, the role of neurons lacking the HCN channels should not be underestimated in comparison with cells possessing them, since in MS the activity of former neurons occurs

after the local field potential (theta rhythm), while the latter start to fire beforehand (Hangya et al. 2009).

In conclusion, a similar bursting activity in the presence of nicotine, to our knowledge, has not been reported previously in the septal structure in general and in LS in particular. Based on similarly affected parameters of evoked (Kodirov et al. 2014) and spontaneous APs, we suggest the role of HCN channels in this modulation.

Materials and Methods

Slice Preparation

The brain was sliced at the coronal plane with a vibrotome and their thicknesses were adjusted to 300 μm (Kodirov et al. 2010). The age of rats ranged from P21 to P46 (P35.4 ± 2.8, $n = 12$) and all underwent anesthesia with isoflurane according the guidelines of the local committee.

Electrophysiology

All patch-clamp experiments were conducted in whole-cell current-clamp mode (Hamill et al. 1981; Krishtal 2015) at room temperature (~22°C). Particular neurons for recordings were chosen in the dorsal part of the LS adjacent to ventricles (Fig. 1). Although the lateral and medial septum (MS), and properties of their neurons are distinct both anatomically and electrophysiologically (Kodirov, unpublished), recordings from cells in the border zone were avoided. The electrode resistance was kept below 6 MΩ in order to enhance the patch quality. Action potentials (AP) were either recorded at or triggered from resting membrane potential (RMP), by incremental injections of current of up to 300 pA, since brain slices were from adult rats. We did not compensate for the series resistance. The input resistance was calculated from voltage deflections during hyperpolarizing steps for all neurons (237.7 ± 17.2 MΩ, $n = 20$), except for one that was subjected to spontaneous AP recording only. External solution included (in mM) 119 NaCl, 2.5 KCl, 1.25 NaH_2PO_4, 1 $MgSO_4$, 2.5 $CaCl_2$, 26 $NaHCO_3$, 10 glucose, and was equilibrated with 95 % O_2 and 5 % CO_2. We could reliably use this solution (albeit cooling) also for the isolation of brain, its slicing, and maintaining sections up to ~8 h. The pipette solution contained (in mM) 120 K^+-gluconate, 5 NaCl, 1 $MgCl_2$, 10 HEPES, 0.2 EGTA, 2 Mg_2ATP, 0.2 NaGTP (pH = 7.2). Nicotine was obtained in liquid form from Sigma. The tested concentrations of nicotine ranged between 300 nM and 3 μM, and in most cases cumulative doses were applied. Although the frequency of spikes is low in LS, we have used relatively faster sampling intervals (5 kHz) in order to fully resolve them. The instantaneous frequencies of both spontaneous and evoked APs were estimated as the inverse of the inter-spike intervals. Values for each parameter of spontaneous spikes are represented by vertical bars and correspond to recordings in a real time for indicated times (at least 1 min). The average data are supplemented with the corresponding SEM. Comparison was made with student's *t* test and values are indicated in "Results" section.

Acknowledgments

The outlined research was supported by National Institute of Health. All authors appreciate the animal care and rats provided by Jennifer Bagley. We thank Boris Ermolinsky for discussions in regard to presented results and tested ideas, Raul Consunji for careful reading, and Morris Benveniste for critiques on the first draft of manuscript. Rosa Marie Pearson enthusiastically co-participated during several experiments.

Abbreviations

LS	Lateral septum
HCN	Hyperpolarization-activated cyclic nucleotide gated non-selective cation channels
RTP	Rebound tail potential
nAChRs	Nicotinic acetylcholine receptors

References

Adams BEL, Reid CA, Myers D, Ng C, Powell K, Phillips AM, Zheng T, O'Brien TJ, Williams DA. Excitotoxic-mediated transcriptional decreases in HCN2 channel function increase network excitability in CA1. Exp Neurol. 2009; 219:249–257. [PubMed: 19500574]

Angelo K, Margrie TW. Population diversity and function of hyperpolarization-activated current in olfactory bulb mitral cells. Sci Rep. 2011; 1:50. [PubMed: 22355569]

Arimitsu T, Nuriya M, Ikeda K, Takahashi T, Yasui M. Activity-dependent regulation of HCN1 protein in cortical neurons. Biochem Biophys Res Commun. 2009; 387:87–91. [PubMed: 19563776]

Bancila V, Cordeiro JM, Bloc A, Dunant Y. Nicotine-induced and depolarisation-induced glutamate release from hippocampus mossy fibre synaptosomes: two distinct mechanisms. J Neurochem. 2009; 110:570–580. [PubMed: 19457080]

Bender RA, Galindo R, Mameli M, Gonzalez-Vega R, Valenzuela CF, Baram TZ. Synchronized network activity in developing rat hippocampus involves regional hyperpolarization-activated cyclic nucleotide-gated (HCN). channel function. Eur J Neurosci. 2005; 22:2669–2674. [PubMed: 16307610]

Blethyn KL, Hughes SW, Toth TI, Cope DW, Crunelli V. Neuronal basis of the slow (\1 Hz). oscillation in neurons of the nucleus reticularis thalami in vitro. J Neurosci. 2006; 26:2474–2486. [PubMed: 16510726]

Brager DH, Lewis AS, Chetkovich DM, Johnston D. Short- and long-term plasticity in CA1 neurons from mice lacking h-channel auxiliary subunit TRIP8b. J Neurophysiol. 2013; 110:2350–2357. [PubMed: 23966674]

Brauer AU, Savaskan NE, Kole MHP, Plaschke M, Monteggia LM, Nestler EJ, Simburger EVA, Deisz RA, Ninnemann O, Nitsch R. Molecular and functional analysis of hyperpolarization-activated pacemaker channels in the hippocampus after entorhinal cortex lesion. FASEB J. 2001; 15:2689–2701. [PubMed: 11726545]

Campanac E, Hoffman DA. Repeated cocaine exposure increases fast-spiking interneuron excitability in the rat medial prefrontal cortex. J Neurophysiol. 2013; 109:2781–2792. [PubMed: 23486201]

Carette B. Noradrenergic responses of neurones in the mediolateral part of the lateral septum: α1-adrenergic depolarization and rhythmic bursting activities, and α2-adrenergic hyperpolarization from guinea pig brain slices. Brain Res Bull. 1999; 48:263–276. [PubMed: 10229333]

Changeux JP. Nicotinic receptors and nicotine addiction. C R Biol. 2009; 332:421–425. [PubMed: 19393973]

Cisse RS, Krebs-Kraft DL, Parent MB. Septal infusions of the hyperpolarization-activated cyclic nucleotide-gated channel (HCN-channel). blocker ZD7288 impair spontaneous alternation but not inhibitory avoidance. Behav Neurosci. 2008; 122:549–556. [PubMed: 18513125]

D'Agostino M, Crespi A, Polishchuk E, Generoso S, Martire G, Colombo S, Bonatti S. ER reorganization is remarkably induced in COS-7 cells accumulating transmembrane protein receptors not competent for export from the endoplasmic reticulum. J Membr Biol. 2014; 247:1149–1159. [PubMed: 25086772]

Day M, Carr DB, Ulrich S, Ilijic E, Tkatch T, Surmeier DJ. Dendritic excitability of mouse frontal cortex pyramidal neurons is shaped by the interaction among HCN, Kir2, and K_{leak} channels. J Neurosci. 2005; 25:8776–8787. [PubMed: 16177047]

Dibattista M, Mazzatenta A, Grassi F, Tirindelli R, Menini A. Hyperpolarization-activated cyclic nucleotide-gated channels in mouse vomeronasal sensory neurons. J Neurophysiol. 2008; 100:576–586. [PubMed: 18509074]

DiFrancesco D, Porciatti F, Janigro D, Maccaferri G, Mangoni M, Tritella T, Chang F, Cohen IS. Block of the cardiac pacemaker current (If). in the rabbit sino-atrial node and in canine Purkinje fibres by 9-amino-1,2,3,4-tetrahydroacridine. Pflugers Arch. 1991; 417:611–615. [PubMed: 2057325]

Fisher JL, Dani JA. Nicotinic receptors on hippocampal cultures can increase synaptic glutamate currents while decreasing the NMDA-receptor component. Neuropharmacology. 2000; 39:2756–2769. [PubMed: 11044745]

Freund TF, Antal M. GABA-containing neurons in the septum control inhibitory interneurons in the hippocampus. Nature. 1988; 336:170–173. [PubMed: 3185735]

Görlich A, Antolin-Fontes B, Ables JL, Frahm S, Slimak MA, Dougherty JD, Ibañez-Tallon I. Reexposure to nicotine during withdrawal increases the pacemaking activity of cholinergic habenular neurons. Proc Natl Acad Sci USA. 2013; 110:17077–17082. [PubMed: 24082085]

Hamill OP, Marty A, Neher E, Sakmann B, Sigworth FJ. Improved patch-clamp techniques for high-resolution current recording from cells and cell-free membrane patches. Pflugers Arch. 1981; 391:85–100. [PubMed: 6270629]

Hangya B, Borhegyi Z, Szilagyi N, Freund TF, Varga V. GABAergic neurons of the medial septum lead the hippocampal network during theta activity. J Neurosci. 2009; 29:8094–8102. [PubMed: 19553449]

Klaassen A, Glykys J, Maguire J, Labarca C, Mody I, Boulter J. Seizures and enhanced cortical GABAergic inhibition in two mouse models of human autosomal dominant nocturnal frontal lobe epilepsy. Proc Natl Acad Sci USA. 2006; 103:19152–19157. [PubMed: 17146052]

Koch U, Grothe B. Hyperpolarization-activated current (I_h). in the inferior colliculus: distribution and contribution to temporal processing. J Neurophysiol. 2003; 90:3679–3687. [PubMed: 12968010]

Kodirov, SA. Targets of addictive nicotine in neurons and different regions of the CNS—amygdala, cerebellum, cortex, hippocampus, hypothalamus, raphe nucleus, septum, striatum, brainstem, and spinal cord—and interactions with alcohol. In: Preedy, VP., editor. The neuropathology of drug addictions and substance misuse. Elsevier; London: 2015.

Kodirov SA, Takizawa S, Joseph J, Kandel ER, Shumyatsky GP, Bolshakov VY. Synaptically released zinc gates long-term potentiation in fear conditioning pathways. Proc Natl Acad Sci USA. 2006; 103:15218–15223. [PubMed: 17005717]

Kodirov SA, Jasiewicz J, Amirmahani P, Psyrakis D, Bonni K, Wehrmeister M, Lutz B. Endogenous cannabinoids trigger the depolarization-induced suppression of excitation in the lateral amygdala. Learn Mem. 2010; 17:832–838.

Kodirov SA, Wehrmeister M, Colom LV. Modulation of HCN channels in lateral septum by nicotine. Neuropharmacology. 2014; 81:274–282. [PubMed: 24582613]

Kolaj M, Zhang L, Renaud LP. Novel coupling between TRPC-like and KNa channels modulates low threshold spike-induced after potentials in rat thalamic midline neurons. Neuropharmacology. 2014; 86:88–96. [PubMed: 25014020]

Kononenko NI, Berezetskaya NM. Modeling the spontaneous activity in suprachiasmatic nucleus neurons: role of cation single channels. J Theor Biol. 2010; 265:115–125. [PubMed: 20362589]

Krishtal O. Receptor for protons: first observations on acid sensing ion channels. Neuropharmacology. 2015; 94:4–8. [PubMed: 25582296]

Lewis AS, Vaidya SP, Blaiss CA, Liu Z, Stoub TR, Brager DH, Chen X, Bender RA, Estep CM, Popov AB, Kang CE, Van Veldhoven PP, Bayliss DA, Nicholson DA, Powell CM, Johnston D,

Chetkovich DM. Deletion of the hyperpolarization-activated cyclic nucleotide-gated channel auxiliary subunit TRIP8b impairs hippocampal I_h localization and function and promotes antidepressant behavior in mice. J Neurosci. 2011; 31:7424–7440. [PubMed: 21593326]

Luthi A, McCormick DA. H-current: properties of a neuronal and network pacemaker. Neuron. 1998; 21:9–12. [PubMed: 9697847]

Magee JC. Dendritic I_h normalizes temporal summation in hippocampal CA1 neurons. Nat Neurosci. 1999; 2:508–514. [PubMed: 10448214]

Mameli-Engvall M, Evrard A, Pons Sp, Maskos U, Svensson TH, Changeux J-P, Faure P. Hierarchical control of dopamine neuron-firing patterns by nicotinic receptors. Neuron. 2006; 50:911–921. [PubMed: 16772172]

Mao B-Q, MacLeish PR, Victor JD. Role of hyperpolarization-activated currents for the intrinsic dynamics of isolated retinal neurons. Biophys J. 2003; 84:2756–2767. [PubMed: 12668483]

Marcelin B, Chauviere L, Becker A, Migliore M, Esclapez M, Bernard C. h channel-dependent deficit of theta oscillation resonance and phase shift in temporal lobe epilepsy. Neurobiol Dis. 2009; 33:436–447. [PubMed: 19135151]

Matsuo R, Kobayashi S, Wakiya K, Yamagishi M, Fukuoka M, Ito E. The cholinergic system in the olfactory center of the terrestrial slug *Limax*. J Comp Neurol. 2014; 522:2951–2966. [PubMed: 24523205]

McRae-Degueurce A, Booj S, Haglid K, Rosengren L, Karlsson JE, Karlsson I, Wallin A, Svennerholm L, Gottfries CG, Dahlstrom A. Antibodies in cerebrospinal fluid of some Alzheimer disease patients recognize cholinergic neurons in the rat central nervous system. Proc Nat Acad Sci USA. 1987; 84:9214–9218. [PubMed: 3321070]

Nazzari H, Angoli D, Chow SS, Whitaker G, Leclair L, McDonald E, Macri V, Zahynacz K, Walker V, Accili EA. Regulation of cell surface expression of functional pacemaker channels by a motif in the B-helix of the cyclic nucleotide-binding domain. Am J Physiol Cell Physiol. 2008; 295:C642–C652. [PubMed: 18614814]

Noble D, Tsien RW. The kinetics and rectifier properties of the slow potassium current in cardiac Purkinje fibres. J Physiol. 1968; 195:185–214. [PubMed: 5639799]

Pal B, Por A, Szucs G, Kovacs I, Rusznak Z. HCN channels contribute to the intrinsic activity of cochlear pyramidal cells. Cell Mol Life Sci. 2003; 60:2189–2199. [PubMed: 14618265]

Ponterio G, Tassone A, Sciamanna G, Riahi E, Vanni V, Bonsi P, Pisani A. Powerful inhibitory action of mu opioid receptors (MOR). on cholinergic interneuron excitability in the dorsal striatum. Neuropharmacology. 2013; 75:78–85. [PubMed: 23891638]

Porter JT, Cauli B, Tsuzuki K, Lambolez B, Rossier J, Audinat E. Selective excitation of subtypes of neocortical interneurons by nicotinic receptors. J Neurosci. 1999; 19:5228–5235. [PubMed: 10377334]

Racine RJ, Milgram NW, Hafner S. Long-term potentiation phenomena in the rat limbic forebrain. Brain Res. 1983; 260:217–231. [PubMed: 6299454]

Ranck JB Jr. Studies on single neurons in dorsal hippocampal formation and septum in unrestrained rats: part I. Behavioral correlates and firing repertoires. Exp Neurol. 1973; 41:462–531.

Rozario AO, Turbendian HK, Fogle KJ, Olivier NB, Tibbs GR. Voltage-dependent opening of HCN channels: facilitation or inhibition by the phytoestrogen, genistein, is determined by the activation status of the cyclic nucleotide gating ring. Biochim Biophys Acta. 2009; 1788:1939–1949. [PubMed: 19524546]

Solomon JS, Doyle JF, Burkhalter A, Nerbonne JM. Differential expression of hyperpolarization-activated currents reveals distinct classes of visual cortical projection neurons. J Neurosci. 1993; 13:5082–5091. [PubMed: 8254362]

Thomas E, Burock D, Knudsen K, Deterding E, Yadin E. Single unit activity in the lateral septum and central nucleus of the amygdala in the elevated plus-maze: a model of exposure therapy? Neurosci Lett. 2013; 548:269–274. [PubMed: 23769728]

Thon S, Schmauder R, Benndorf K. Elementary functional properties of single HCN2 channels. Biophys J. 2014; 105:1581–1589.

Thuault SJ, Malleret G, Constantinople CM, Nicholls R, Chen I, Zhu J, Panteleyev A, Vronskaya S, Nolan MF, Bruno R, Siegelbaum SA, Kandel ER. Prefrontal cortex HCN1 channels enable

intrinsic persistent neural firing and executive memory function. J Neurosci. 2013; 33:13583–13599. [PubMed: 23966682]

Tokay T, Rohde M, Krabbe S, Rehberg M, Bender RA, Kohling R, Kirschstein T. HCN1 channels constrain DHPG-induced LTD at hippocampal Schaffer collateral-CA1 synapses. Learn Mem. 2009; 16:769–776. [PubMed: 19940037]

Toth K, Freund TF, Miles R. Disinhibition of rat hippocampal pyramidal cells by GABAergic afferents from the septum. J Physiol. 1997; 500:463–474. [PubMed: 9147330]

van den Hooff P, Urban IJ, de Wied D. Vasopressin maintains long-term potentiation in rat lateral septum slices. Brain Res. 1989; 505:181–186. [PubMed: 2532055]

van Welie I, Wadman WJ, van Hooft JA. Low affinity block of native and cloned hyperpolarization-activated I_h channels by Ba^{2+} ions. Eur J Pharmacol. 2005; 507:15–20. [PubMed: 15659289]

Vasilyev DV, Shan Q, Lee Y, Mayer SC, Bowlby MR, Strassle BW, Kaftan EJ, Rogers KE, Dunlop J. Direct inhibition of I_h by analgesic loperamide in rat DRG neurons. J Neurophysiol. 2007; 97:3713–3721. [PubMed: 17392420]

Vassalle M, Yu H, Cohen IS. The pacemaker current in cardiac Purkinje myocytes. J Gen Physiol. 1995; 106:559–578. [PubMed: 8786348]

Velumian AA, Zhang L, Pennefather P, Carlen PL. Reversible inhibition of I_K, I_{AHP}, I_h and I_{Ca} currents by internally applied gluconate in rat hippocampal pyramidal neurones. Pflugers Arch. 1997; 433:343–350. [PubMed: 9064651]

Vinogradova OS. Hippocampus as comparator: role of the two input and two output systems of the hippocampus in selection and registration of information. Hippocampus. 2001; 11:578–598. [PubMed: 11732710]

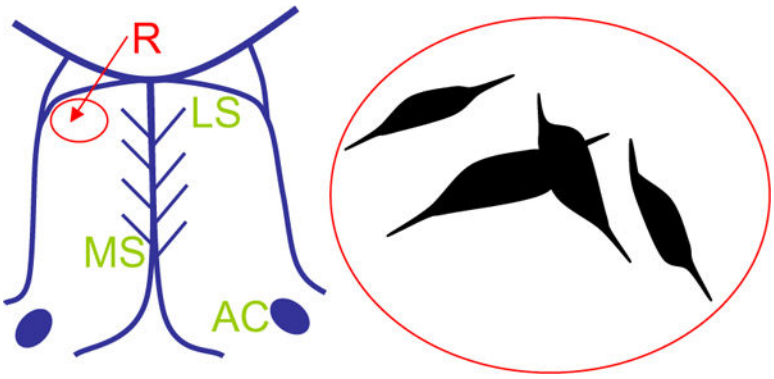

Fig. 1.

Schematic drawing of the appearances of recorded slices and neurons from the protocol: page 91, slice number 3, cell number 08d23100. Data from this neuron are presented in Fig. 11. *R* recording site for majority of cells, *MS* medial septum, *LS* lateral septum, *AC* anterior commissure

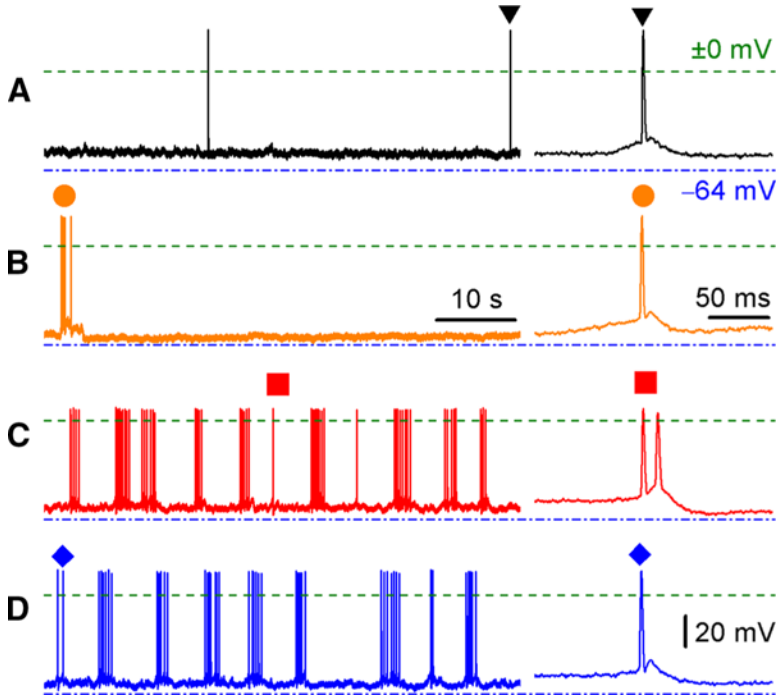

Fig. 2.

Spontaneous action potentials in LS neuron. APs were recorded under control conditions (**a**), after treatment with 1 μM (**b**), 3 μM nicotine (**c**), and upon its wash-out (**d**). Randomly selected APs for all four conditions are shown in *right panels* in an expanded time scale. Note that in the presence of nicotine most of bursts start with “double spikes” as shown in **c**. The same tendency remains during wash-out and the waveform of 3rd AP in **d** is similar to a single AP in **a**, albeit the increased ADP (see Fig. 6). However, the bursting behavior is independent of double spiking (see Figs. 3, 4). *Upper* and *lower dashed lines* indicate identical ±0 and −64 mV (closely corresponds to RMP) levels, respectively. An identical amplitude *scale bars* apply for (**a**–**d**). *Time scales* are identical for main panels and corresponding *insets*

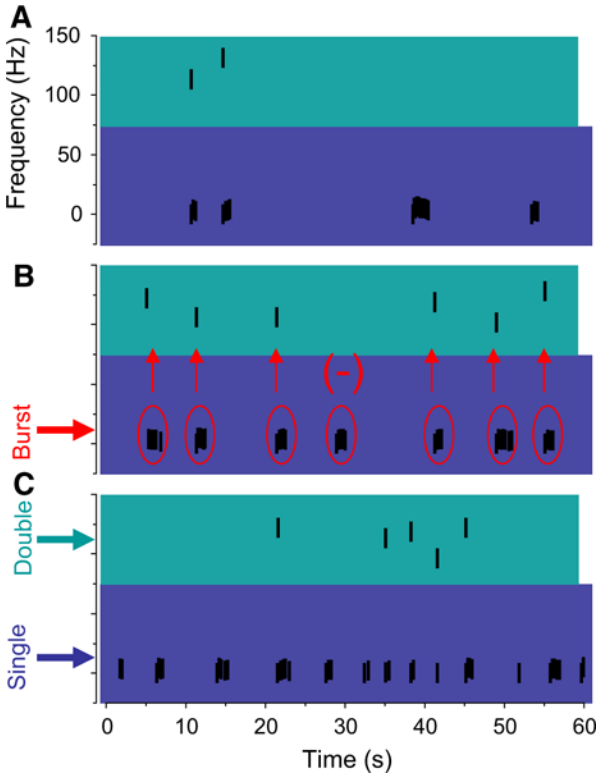

Fig. 3.

Instantaneous frequency of spontaneous APs in the presence of nicotine. Each *vertical bar* represents an AP. The bursting behavior can be also appreciated by plotting frequencies of spikes over 60 s segments. **a**–**c** correspond to the time points of exposure to 3 μM nicotine at 9, 14, and 18 min, respectively. Experiments reveal a major diapason around 1 Hz compared to secondary one at ~100 Hz that corresponds to the frequency of 2nd spikes (*red-colored up arrow*). For clarity the frequency diapasons of 1st and 2nd spikes are color matched (**a**–**c**). Examples of regular bursting are *circled* in **b** and in 6 out of these 7 bursts accompanying 2nd spikes are observed (Color figure online)

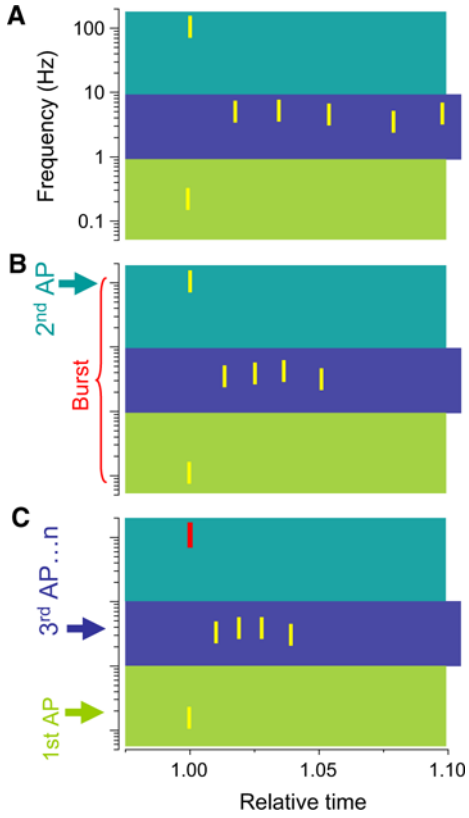

Fig. 4.

Instantaneous frequency of spontaneous SWB. All capital letters (**a**–**c**) respectively correspond to 1st, 2nd, and 3rd bursts observed during continuous recording. As it is evidenced the absence of 2nd spike (**I**, **c**) does not influence the sequential frequency diapason (1–10 Hz) of subsequent APs within bursts. This diapason is a middle range compared to that of the 1st (0.1–1 Hz) and the 2nd (100–200 Hz) spikes (Color figure online)

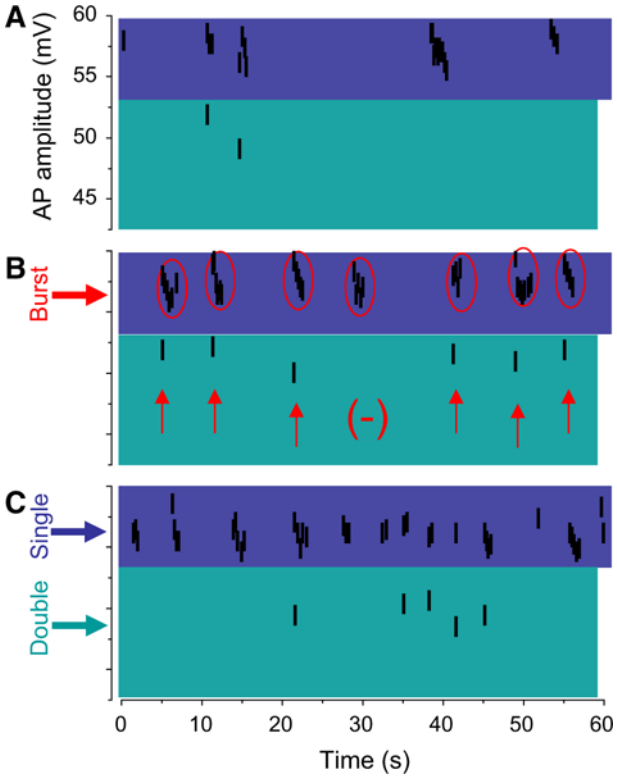

Fig. 5.

Amplitude dynamics. Bursting behavior is reflected by amplitude values of sequential spikes (**a**–**c**). As a rule the amplitude of 2nd spike in case of “double spikes” is lower than the 1st one. Their premature origin is depicted in Fig. 6. For adequate comparison of amplitude and frequency behaviors the same segments from Fig. 3 are analyzed and bursting patterns are *circled*. Note the increased variability in amplitudes of single and occasional 2nd spikes compared to their frequencies

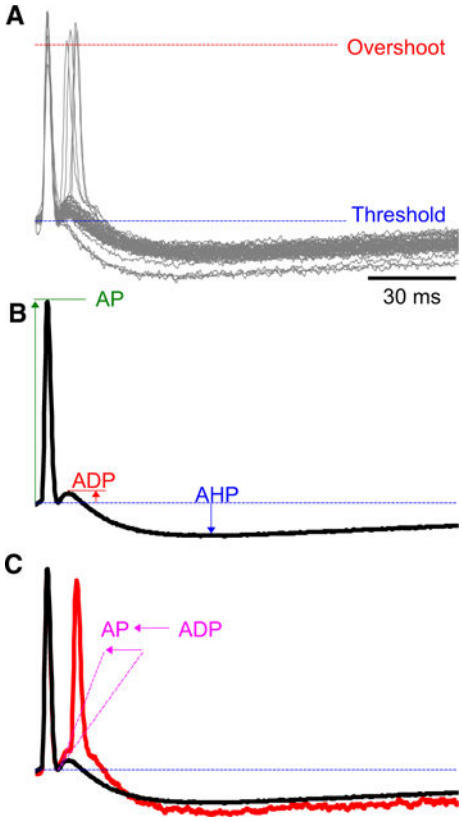

Fig. 6.

ADP to spike transition. **a** Parameters of spontaneous spikes (n = 51) in the presence of nicotine. Overshoot potential and mean threshold values are indicated. **b** Average trace of 47 single spikes from (**a**). In this neuron the ADP is followed by a slow AHP lasting for more than 150 ms. Estimation of amplitudes of spikes (AP), ADP, and AHP are performed as shown. **c** One of the “double spikes” is superimposed with the average trace of single spikes shown in **b**. The maximal slope of rising phase of ADP was 1.4 mV/ms after single spikes. During the transition into the premature spike, the slope of ADP increased to 3 mV/ms. The accelerated slope is paralleled by an increase in amplitude (2.5 vs. 5.6 mV), and some of ADP subsequently triggered the 2nd spike. Note that the 2nd spikes do not possess ADP, but their AHP phase is increased in amplitude (see Fig. 7)

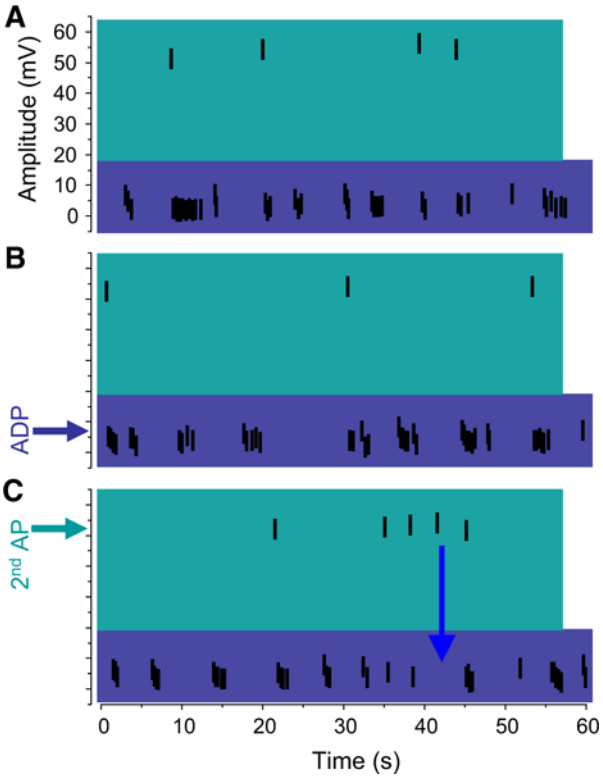

Fig. 7.

The presence of ADP reflects a consistent bursting behavior. **a**–**c** The amplitude of ADP for each single SWB was calculated as indicated in Fig. 6. Data are presented for continuous recordings during 5 min. Note that for comparison purpose the amplitudes of 2nd APs are also plotted. The latter also reveals if the ADP is absent (**c**) when the double spiking occurs (*blue-colored down arrow*) (Color figure online)

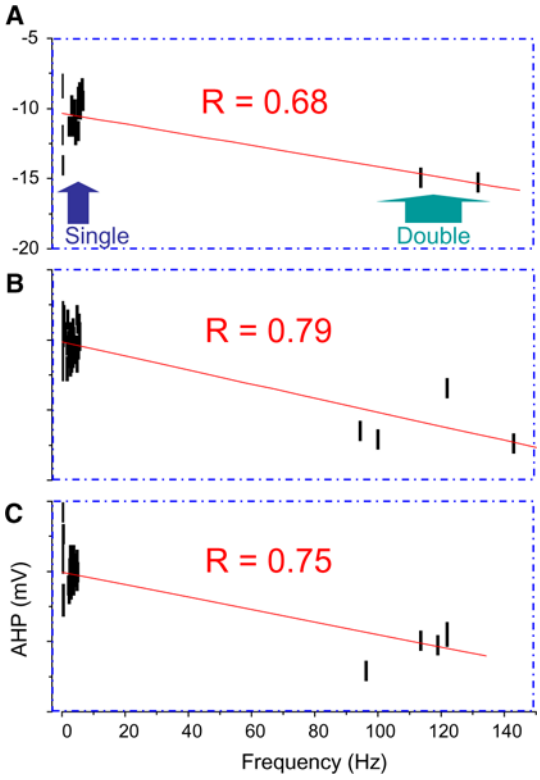

Fig. 8.

The relationship between AHP amplitude and spike frequency was linear. The amplitude of AHP clearly depends on whether or not it was triggered by either single or double spikes (see also Fig. 6). AHP triggered by single AP has a narrow diapason, while those by double spikes have a broader range. The linear relationship ($Y = A ? B * X$) remained similar under these conditions

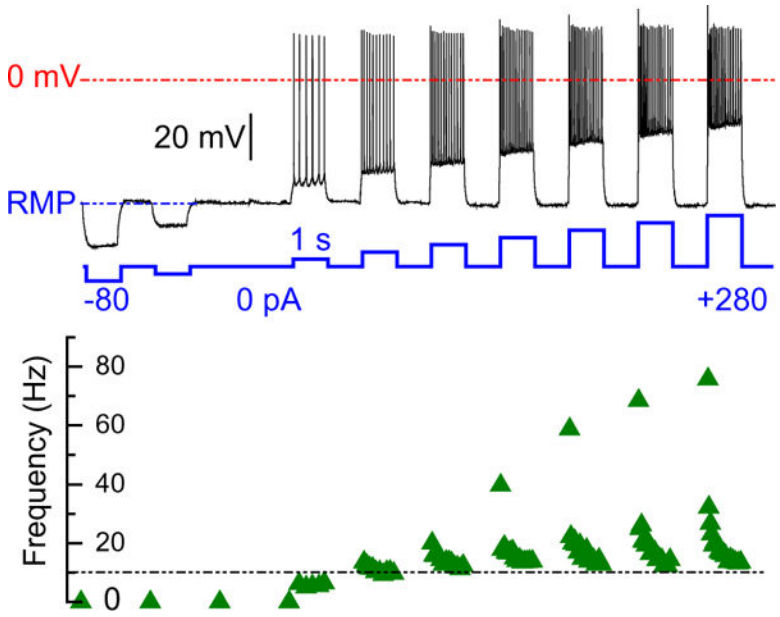

Fig. 9.

Frequency of the evoked double spikes. MP responses to incremental (40 pA) current injections (from −80 to 280 pA) are shown. Easy manifestation of double spiking was achieved based on instantaneous frequencies. The frequency of evoked APs during constant steps increases according to injected current magnitude, and double spikes occur only at more depolarized MP starting at 160 pA. The double spiking occurs at gradually higher rates according to the magnitude of injected currents. Thereafter, a rapid adaptation in frequency of 3rd and subsequent APs is seen. The rate stabilizes at ~10 Hz during each step. Calculation is performed for total of 99 APs, which includes also 4 double spikes

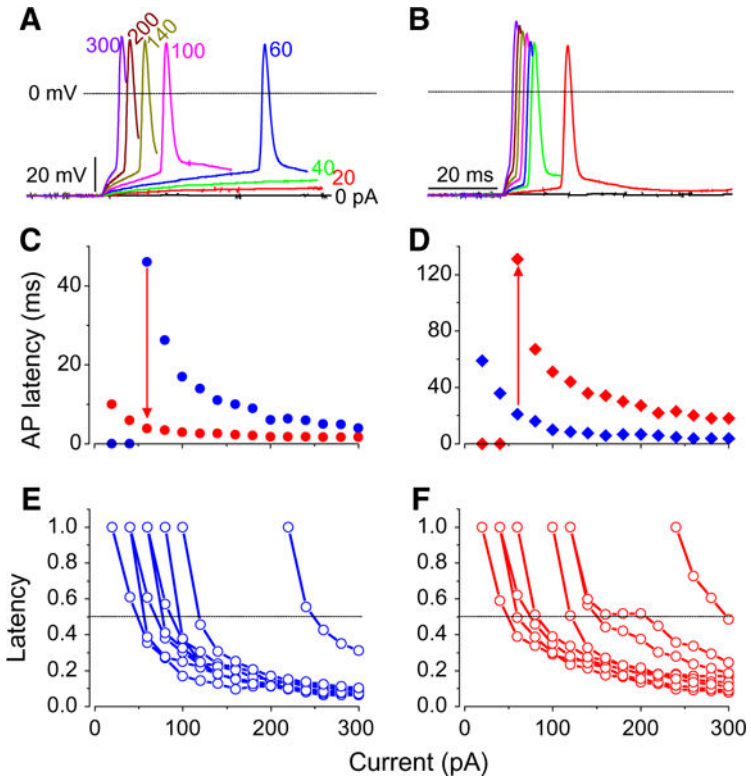

Fig. 10.

Action potential latencies in LS neurons. **a** The evoked APs by somatic current injections of different magnitudes (*color* coded and shown next to APs) are superimposed. The beginning of the overshoot phase of APs is indicated by the line at ±0 mV. RMP was −56 mV. No APs were triggered at 20 and 40 pA in standard ACSF. **b** The exposure of same neuron to 3 μM nicotine. The APs are color matched with respect to those in **a**. **c** The latency values at 20–300 pA under control conditions (*blue-colored circle*) and in the presence of nicotine (*red-colored circle*). In the presence of nicotine APs are triggered even at 20 and 40 pA, and latencies at each current magnitude are significantly decreased (*red-colored down arrow*). Raw data are shown in **a**, **b**, respectively. **d** The representative latency values from a single neuron that belongs to the group in which nicotine suppressed the excitability. Note a complete abolishment of APs at 20 and 40 pA and a significant increase (*red-colored up arrow*) in latencies at more depolarized states. **e**, **f** Normalized values for all individual neurons in the absence and presence of nicotine ($n = 8$). Under control conditions, the overall ratio along the current magnitude has decreased faster than those in the presence of nicotine. Importantly, the ratio between the first and 2nd injected current magnitudes was ~50 % and gradually decreased further to more stable values. *Scale bars* for **a** and **b** are identical (Color figure online)

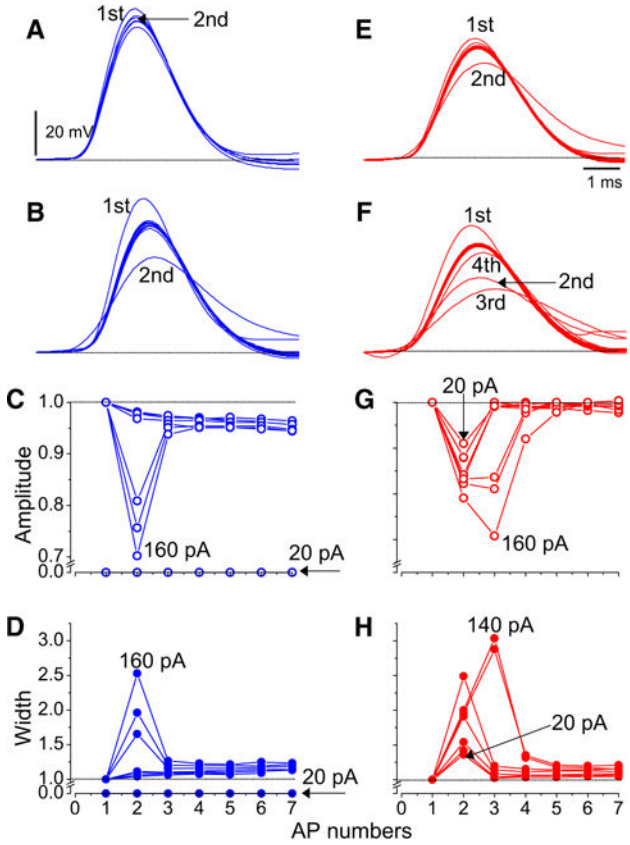

Fig. 11.

Distinct firing pattern of LS neurons and facilitation of excitability by nicotine. **a**, **b** The superimposed APs evoked by 1 s depolarizing currents of 40 and 140 pA magnitudes, respectively. All cells were excited from RMP. **c** Normalized amplitude values for data points collected at 20–160 pA during the same experiment shown in **a**, **b**. The neuron did not respond with APs during 20 pA current injection. **d** The mirror correlations of normalized half-width values to those of amplitudes at each injected current magnitude. Note a similar gradual decrease in amplitudes and half-widths estimated for the initial seven APs. **e**, **f** Evoked APs in the presence of 3 μM nicotine in the same neuron. Note a decrease in the amplitude of 2nd AP at 40 pA (**e**) and even 4th one at 140 pA (**f**). **g** Relative amplitude values from this neuron now reveal both the generation of APs at 20 pA and complex responses during further depolarization. **h** Similar to amplitude values also the half-width was dependent on the AP sequence during each step in the presence of nicotine. However, effects were more severe in regard to half-width, and therefore, in this neuron the values can not reliably estimated at 160 pA

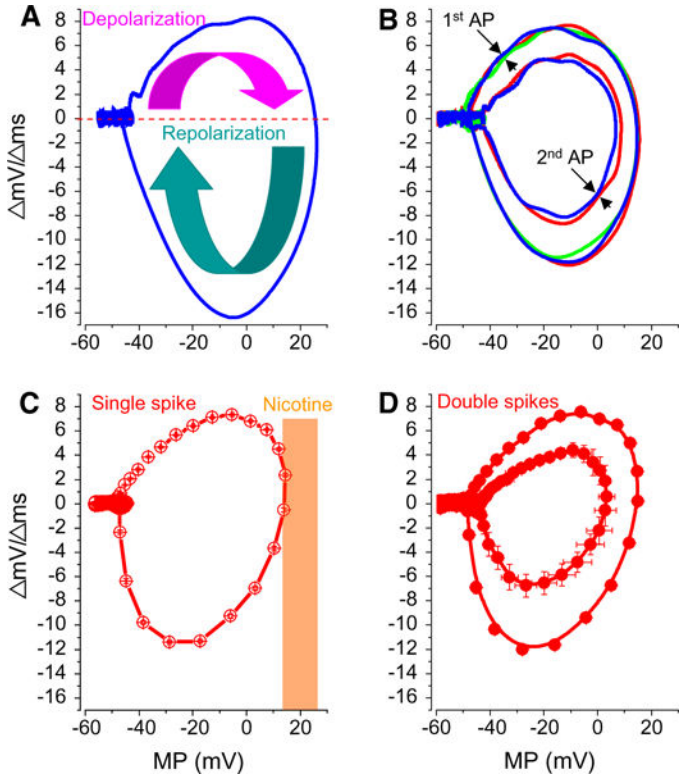

Fig. 12.

Decreased overshoot potential in the presence of nicotine. **a** Temporal changes of MP during spontaneous action potentials under control conditions. The beginning of the trace at ±0ΔmV/Δms corresponds to RMP of −55.2 mV. **b** Three superimposed APs in the same neuron after application of nicotine. In two of them double spiking (2nd AP) was observed. **c** Average values of single spikes (n = 35). Note that the nicotine decreased the overshoot potential and the extent (*vertical bar*) is shown in reference to the control value in **a**. SEM are small and simultaneously shown for both ΔmV/Δms and MP. **d** The rate of double spikes (n = 10). The time courses of depolarization and repolarization for the 1st AP are similar whether a neuron generates single (**c**) or double spikes (**d**). The ΔmV/Δms of 2nd AP during the double spiking are slower, but the gradual changes almost mirror those of the 1st AP